



Journal Name

## COMMUNICATION

# Simultaneous Activity and Surface Area Measurements on Single Mesoporous Nanoparticle Aggregates

Received 00th January 20xx,  
Accepted 00th January 20xx

Xue Jiao<sup>a</sup>, Christopher Batchelor-McAuley<sup>a</sup>, Neil P. Young<sup>b</sup>, and Richard G. Compton<sup>a\*</sup>

DOI: 10.1039/x0xx00000x

www.rsc.org/

**The underpotential deposition and removal of hydrogen from a mesoporous platinum nanoparticle surface is shown to quantify the electroactive surface area of an *individual* nanoparticle. This surface area of the particle is concomitantly correlated with its individual catalytic activity (current density) towards the evolution of hydrogen.**

Use of stochastic nanoparticle analysis methodologies enables the heterogeneity inherent in a sample population to be experimentally probed.<sup>1</sup> Over the preceding decade the electrochemical study of individual nanoparticles has become an active area of development.<sup>2–5</sup> This work gives insight into the specific structure/activity relationship of the catalytic material. Although measurements are made on individual entities, correlation of this data with other information obtained ex-situ can generally only be achieved on a statistical basis. To overcome this challenge work has sought to combine both optical<sup>6</sup> and electron<sup>7</sup> microscopy techniques to enable in-situ monitoring of reactions at the nanoscale. We now show that current-time transients recorded for particle impacts on electrode allow the simultaneous measurement of catalytic activity and particle surface area.

The technique of Faradaic single particle electrochemical impacts, also known as “nanoimpacts”, may be broadly divided into two main types:<sup>8–10</sup> first, a catalytic reaction *mediated* by the nanoparticle can provide information about the particle’s catalytic activity;<sup>2,11</sup> second, a *direct* redox reaction of the particle can be driven, yielding information about the particle’s properties.<sup>12–13</sup> These two approaches provide complementary information regarding the reactions occurring at the nanoscale.

A key factor in the study of heterogeneous redox reactions is knowledge of the electrochemically active surface area

(ECSA).<sup>14</sup> For platinum surfaces at the macroscale measurement of the ECSA is commonly attained by determining the charge passed when a monolayer of an electroadsorbed species such as carbon monoxide, hydrogen or iodine is electrochemically<sup>15</sup> removed from the metallic surface. It is through the measurement of the ECSA of *ensembles* of particles that the *specific* current densities of new oxygen reduction reaction catalysts are routinely experimentally determined.<sup>16–17</sup>

Many previous studies have reported the detection of single nanoparticles by collision with microelectrodes including platinum particles.<sup>18</sup> However in this work for the first time, it is demonstrated how a single nanoparticle current transient response can *size* the ECSA of a *mesoporous* particle and concomitantly provide a measure of its *catalytic activity* (as quantified *via* the catalytic current density at a set overpotential). The technique is evidenced using the single mesoporous particle catalysis of the hydrogen evolution reaction.<sup>8, 15–16</sup> First, we outline the behaviour and cyclic voltammetric responses of random nanoparticle arrays. Second, at the single particle scale, reductive responses arising from underpotential hydrogen deposition ( $H_{upd}$ ) are revealed in an electrolyte saturated with nitrogen. These values are compared to measurements of the  $H_{upd}$  oxidation in the presence of hydrogen. Third, this  $H_{upd}$  signal is shown to give a direct measure of an individual entity’s ECSA. The determined ECSA distribution for the impacting entities is in excellent agreement with the expected surface areas of individual particles as determined from TEM measurement and recognizing their porosity. This comparison indicates that 70–80% of the electrochemical events are associated with the arrival of *individual* particles.

The nanoparticles used in this work are mesoporous in structure (TEM image Figure 1 a) with an average radius of  $23.1 \pm 2.1$  nm and are individually comprised of aggregates of smaller platinum particles of radii  $2.0 \pm 0.3$  nm (Figure 1 b provides the associated size distributions). From the geometry of such materials, assuming a close-packing structure of the small particles (possibly leading to an overestimation of the

<sup>a</sup> Department of Chemistry, Physical and Theoretical Chemistry Laboratory, University of Oxford, South Parks Road, Oxford OX1 3QZ, United Kingdom.

<sup>b</sup> Department of Materials, University of Oxford, Parks Road, Oxford OX1 3PH, United Kingdom.

\*Electronic Supplementary Information (ESI) available: [details of any supplementary information available should be included here]. See DOI: 10.1039/x0xx00000x

## COMMUNICATION

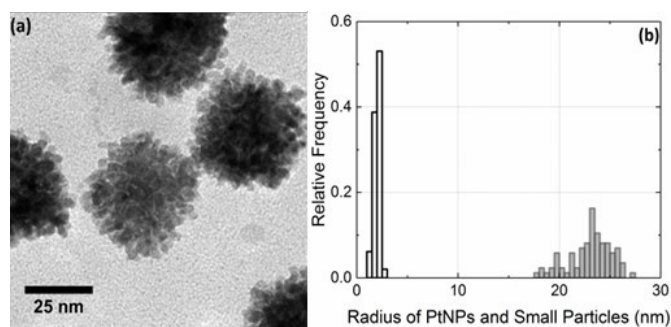


**Figure 1.** (a) Representative TEM image of mesoporous PtNP aggregates. (b) Size distributions of mesoporous PtNPs (grey columns) and small particles (white columns) contained in the aggregate PtNP structure with average radii of  $23.1 \pm 2.1$  nm (of 86 measurements) and  $2.0 \pm 0.3$  nm (of 49 measurements), respectively.

ECSA), the total surface area of these mesoporous aggregates is found to be approximately 8.5 times greater than that of a solid sphere with an equivalent radius of 23.1 nm. SI section 2 presents a UV-vis study of the stability of the nanoparticles in the presence of millimolar electrolyte. The PtNPs are relatively stable within the experimental timescale (<30 mins). For longer times the possible agglomeration of nanoparticle aggregates is indicated by these results, this potential issue is returned to later in the text.

To characterize the activity and electrochemical behavior of the platinum nanoparticles we first look at the electrochemical response of micro arrays of randomly distributed nanoparticles. A gold microelectrode (radius = 5  $\mu\text{m}$ ) was submerged into a PtNP suspension (6.7  $\mu\text{M}$ ) containing 20 mM KOH and saturated with nitrogen. The gold electrode was selected due to the low activity of the material towards the hydrogen evolution reaction (HER). In a degassed solution cyclic voltammetry was conducted from -1.0 to 0.0 V vs Ag/AgCl in 1M KCl (Figure 2). The freely diffusing platinum nanoparticles randomly collide with and adhere to the electrode. Note the nanoparticles have been previously shown to irreversibly adsorb to the electrode surface.<sup>19</sup> Over the course of multiple scans and as PtNP accumulate at the electrochemical substrate a surface bound voltammetric feature becomes observable at *ca.* -0.49 V. This surface bound wave is associated with the underpotential deposition and removal of hydrogen ( $\text{H}_{\text{upd}}$ )<sup>20-21</sup> at the platinum surface. Importantly, the nanoparticles employed in this work are citrate capped, which leads to a different  $\text{H}_{\text{upd}}$  response from that of a bare platinum surface.<sup>22</sup> During the course of the cyclic voltammetric scan reductive spikes in current are also observed. These spikes in current are associated with the arrival of new platinum entities to the electrode surface during the course of the scan. The magnitude of these features was investigated *via* chronamperometry at electrode potentials of -0.60 and -0.70 V (i.e. at potentials positive of the reversible hydrogen electrode), examples of the raw current-time transients can be found in the SI section 3 (Figure S2). Integration of these spikes allowed the charge passed per nano-event to be determined to be *ca.* 0.20 pC (as depicted on Figure 2).

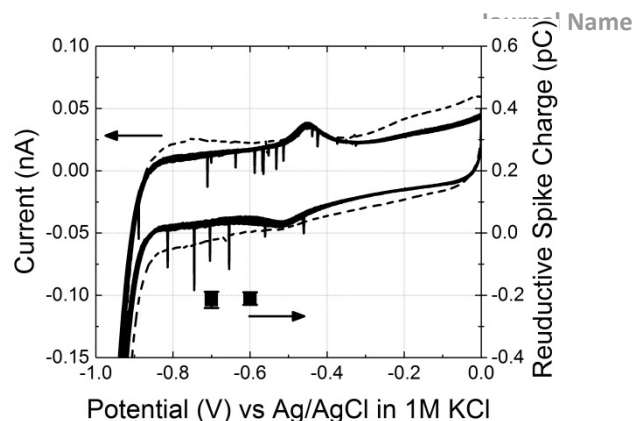
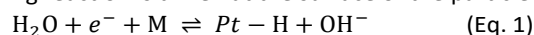


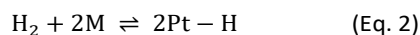
**Figure 2.** Cyclic voltammograms for  $\text{H}_{\text{upd}}$  reduction (black line) on an Au microelectrode with a random array of adsorbed mesoporous PtNPs (CV of scan rate  $200 \text{ mVs}^{-1}$ ; nanoparticle of radius 23.1 nm, electrode of radius 5  $\mu\text{m}$ ). The initial scan is also shown in the diagram (dashed line). Overlaid (right hand side axis) is the current response of individual mesoporous PtNPs as measured by chronoamperometry at -0.60 and -0.70 V (black squares) vs Ag/AgCl in 1 M KCl (measured from the time current transients, 200 ms after the nanoparticle arrival). The electrolyte is 20 mM KOH saturated with  $\text{N}_2$ .

These spikes in current are associated with the deposition of  $\text{H}_{\text{upd}}$  at the newly arriving nanoparticle surface. Upon arrival of a platinum nanoparticle to a cathodically potentiostated electrode (below *ca.* -0.49 V vs Ag/AgCl in 1 M KCl), the following reaction is driven at the surface of the particle:



where M is an unoccupied platinum surface site; hence, the magnitude of this process is sensitive to the nanoparticle's initial  $\text{H}_{\text{upd}}$  surface coverage and its total electroactive surface area. A monolayer coverage of  $\text{H}_{\text{upd}}$  on a platinum surface corresponds to a charge of  $210 \mu\text{C cm}^{-2}$ .<sup>14</sup> Consequently, the charge passed during a single entity reduction event can thus be converted to an effective surface area. Figure 3 shows the cumulative frequency of the measured electroactive surface area per nano-event as measured from the reductive deposition of  $\text{H}_{\text{upd}}$ .

However, as illustrated by the UV-vis measurements (SI section 2), in the solution phase the mesoporous PtNP aggregates are only metastable in the presence of millimolar electrolyte concentrations; moreover, their stability is seemingly lower in the presence of nitrogen as opposed to hydrogen. In order to assess the extent to which the solution phase agglomeration level of the nanoparticle aggregates influences the electrochemical response the oxidation of  $\text{H}_{\text{upd}}$  was investigated. In a solution saturated with hydrogen the platinum nanoparticles become chemically modified with a surface layer of adsorbed  $\text{H}_{\text{upd}}$ , as driven by the reaction below:



Consequently, by chemically tuning the surface functionality of the nanoparticles the influence of the presence of the hydrogen gas can be directly probed. To achieve this a gold microelectrode (10  $\mu\text{m}$  diameter) was immersed under potentiostatic control into an alkaline solution (20 mM KOH) containing mesoporous PtNPs (6.7  $\mu\text{M}$ ) saturated with

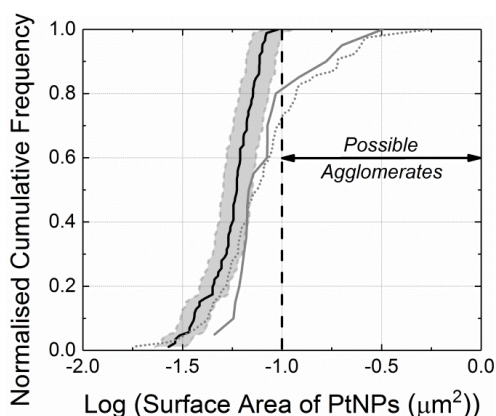


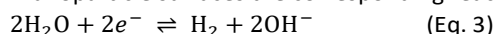
**Figure 3.** Plot of normalised cumulative frequency against surface area of PtNPs on a log scale from TEM (black solid line with grey dash lines to show the upper and lower error estimates),  $H_{\text{upd}}$  reduction at  $-0.60$  V (nitrogen sat., grey dot line) and oxidation at  $0.15$  V (hydrogen sat., grey solid line). A vertical black dash line indicates the threshold above which the impacts may be due to agglomerates, as determined under an assumption of a complete monolayer of  $H_{\text{upd}}$  being added or removed during the course of the electrochemical process.

hydrogen ( $[H_2]_{\text{sat}} = 0.73$  mM)<sup>23</sup>. A potential of  $0.15$  V (vs Ag/AgCl in  $1$  M KCl) was selected for chronoamperometry. Upon impact of the nanoparticles to the electrode, small oxidative spikes were observed in the measured time-current profile. Examples of the voltamogram and the raw current-time transients can be found in the SI section 4 (Figure S3 and S4). These spikes correspond under these conditions to the oxidative removal of  $H_{\text{upd}}$  from the impacting nanoparticle surfaces. Again, the charge passed per impact event can be used to give an estimate of the total electroactive platinum surface area of the impacting entity. The resulting size distribution of the measured single entity platinum surface areas are again presented in Figure 3. The surface area size distribution measured from the oxidative removal of the  $H_{\text{upd}}$  is within experimental error to that obtained for the corresponding reductive deposition process. These two measurements have been performed in solutions containing hydrogen and nitrogen respectively, this subsequently indicates that, over the experimental timescale ( $<30$  minutes), the presence of the gas does not lead to measurably different agglomeration levels of the *impacting* nanoparticles.

To what extent do these single entity surface area measurements reflect the arrival of *individual* nanoparticle aggregates? Figure 3 depicts the predicted surface area cumulative frequency plot for the *individual* particles as determined from TEM. This estimation has been made on the basis of fully accounting for the internal surface area of the mesoporous nanoparticle *ca.* 8.5 times larger surface area than that of a solid sphere of equivalent radius. Once the particles mesoporous structure is considered, good agreement is found between the particle surface area distributions as measured *via* TEM and the nano-impact techniques.<sup>19</sup> This result, first, indicates that the *entire* nanoparticle surface area (internal and external) is electroactive and contributes to the

charge passed during spike of the impact event (see SI section 5 for further details on electrochemical particle surface area measurements). Second, the likely extent of the nanoparticle agglomeration of the *impacting* platinum entities can be evidenced. The electrochemically measured area per entity is marginally higher than that predicted from TEM for a single nanoparticle aggregate (here we are referring to a single mesoporous particle of radius  $23.1$  nm). On the basis of the data shown in Figure 3, it is estimated that over the course of these experiments the impact results are fully consistent with 70-80 % of the events being due to the arrival of a single particle aggregate.

At more negative electrode potentials ( $E_{\text{RHE}} = -0.96$  V vs Ag/AgCl in  $1$  M KCl at pH 12.27) the hydrogen evolution reaction (HER) can be driven to occur at the individual catalytic PtNPs. To study this catalytic process a gold microelectrode was submerged into a nanoparticle suspension containing  $20$  mM KOH and either saturated with nitrogen or hydrogen. PtNPs diffuse, freely collide with and stick on to the gold substrate. Chronoamperograms were recorded at a potential of  $-1.30$  V vs Ag/AgCl in  $1$  M KCl. At this potential no significant hydrogen evolution occurs on the bare gold substrate (see SI section 6, Figure S5). The arrival and impact of a nanoparticle entity at the interface leads to measured steps in the time-current transient. The raw data is shown in the SI section 6. From these individual events the “average” response of multiple individual nano-impact events can be determined, as presented in Figure 4. In both the presence of hydrogen and nitrogen a step in current is recorded which after approximately  $200$  ms has a steady-state current of *ca.*  $25$  pA. This steady-state current gives a direct measure of the rate of catalytic reduction of water at this high pH. At the individual platinum nanoparticle surfaces the corresponding reaction is:



The magnitude of this steady-state catalytic current is sensitive to the applied electrode potential.

Notably, as seen in Figure 4, in the absence of solution phase hydrogen an initial spike in current is observed at the onset of the individual catalytic event (SI Section 6, Figure S6). The addition of hydrogen to the nanoparticle sol suppresses this initial peak in current (SI Section 6, Figure S7). This occurs as, in the solution phase and in the presence of  $H_2$ , the nanoparticles become pre-modified with a monolayer of  $H_{\text{upd}}$  as formed by the chemisorption of the gas to the catalytic surface, as discussed earlier (Equation 2). Consequently, in the absence of solution phase hydrogen this initial spike in current can be used to provide a *direct* measure of an individual impacting entities electroactive surface area. The inlay of Figure 4 depicts for individual nano-impact events the magnitude of the initial spike in current as compared to the resulting catalytic current step size. A strong ( $R^2 = 0.86$ ) positive correlation between these two features is found. For a single PtNP, the maximum surface area predicted is  $\sim 0.1 \mu\text{m}^2$ , consequently nano-impact events with an initial spike larger than this threshold are ascribed as occurring due to the arrival of agglomerated material, as indicated visually in the inlay of Figure 4.

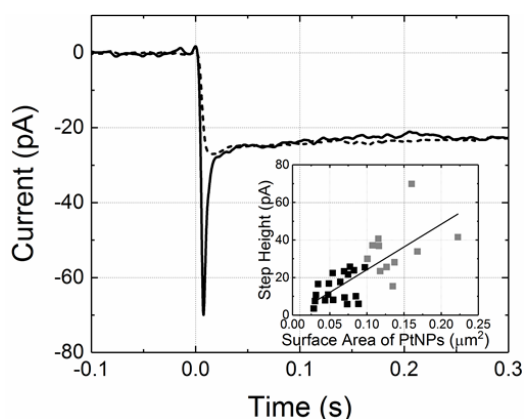


**Figure 4.** Overlay of the averaged HER response of individual mesoporous PtNPs upon arrival, and electrical contact with, a potentiostated Au microelectrode with an applied potential of -1.30 V (vs Ag/AgCl in 1 M KCl). The electrolyte is 20 mM KOH saturated with H<sub>2</sub> (dash line) or N<sub>2</sub> (solid line). Current responses given as a function of time where  $t = 0$  is taken as the nanoparticle arrival and is associated with the step in current. Inset: Plot of surface area of single PtNPs (as calculated on the basis of  $H_{\text{upd}}$  signal of  $210 \mu\text{C cm}^{-2}$ ) against step height of individual impacts (black squares: measured at the time-current transients). Linear fitting of 30 measurements has been forced to pass 0 (black line) with a  $R^2$  value of 0.86.

Through controlling the reaction conditions and undertaking single nanoparticle catalytic reduction reactions either in the presence or absence of hydrogen gas, the surface functionality of the nanoparticles in suspension can be chemically altered. By exploiting this control we can directly evidence that the initial reductive spike in current, as observed for individual nanoparticles, can be unambiguously identified as relating to the formation of a monolayer coverage of  $H_{\text{upd}}$ . Hence, the magnitude of this peak gives a direct measure of the nanoparticle's electroactive surface area. At an intrinsic level such a method, providing simultaneous sizing and activity information, yields a route by which nanoparticulate *specific* activity may be identified in a stochastic manner. In the present case at -1.30 V ( $E_{\text{RHE}} = -0.96$  V vs Ag/AgCl in 1M KCl), the average catalytic *specific* current density for the alkaline evolution of hydrogen at the single particle is determined to be  $242 \pm 18 \text{ A m}^{-2}$  as estimated from the slope of the linear fitting line in the inlay of Figure 4. This is in contrast with the current density on bulk platinum which has been measured to be  $352 \text{ A m}^{-2}$  at -1.30 V (vs Ag/AgCl in 1M KCl) under these experimental conditions (see SI Section 7). This lower activity of the nanoparticulate material may either reflect the nanoparticulate material being inherently lower in activity, be a result of particle's local porous structure, or relate to the electrical connectivity<sup>24</sup> of the particle. Specifically, the reported activity (current density) for the mesoporous particle is a measure of the average rate over the entire nanoparticle structure, including internal and external surfaces. The platinum surface at the centre of the particle is not as accessible as the outer edge of the particle. Hence, there will likely be concentration and potential gradients through the

porous structure of the nanoparticle, plausibly leading, for a given electrode potential, to a lower activity of the platinum at the centre of the mesoporous structure. Alternately, this apparently lower activity may result from electron transport issues either to or through the particle itself.

## Acknowledgements

The research leading to these results has received partial funding from the European Research Council under the European Union's Seventh Framework Programme (FP/2007–2013)/ERC Grant Agreement no. [320403]. X.J. thanks the China Scholarship Council for supporting her DPhil research.

## Conflicts of interest

There are no conflicts to declare.

## Notes and references

- 1 J. J. Gooding. *Angew. Chem. Int. Ed.* 2016, **55**, 12956-12958.
- 2 X. Xiao, A. J. Bard. *J. Am. Chem. Soc.* 2007, **129**, 9610-9612.
- 3 K. J. Stevenson, K. Tschulik. *Curr. Opin. Electrochem.* 2017, **6**, 38-45.
- 4 T. Imaoka, Y. Akanuma, N. Haruta, S. Tsuchiya, K. Ishihara, T. Okayasu, W.-J. Chun; M. Takahashi, K. Yamamoto. *Nat. Commun.* 2017, **8**, 688.
- 5 S. Tahmasebi, G. Jerkiewicz, S. Baranton, C. Coutanceau, Y. Furuya, A. Ohma. *J. Phys. Chem. C* 2018, **122**, 11765-11776.
- 6 W. Wang. *Chem. Soc. Rev.* 2018, **47**, 2485-2508.
- 7 Y. A. Wu, Z. Yin, M. Farmand, Y.-S. Yu, D. A. Shapiro, H.-G. Liao, W.-I. Liang, Y.-H. Chu, H. Zheng. *Sci. Rep.* 2017, **7**, 42527.
- 8 S. V. Sokolov, S. Eloul, E. Katelhon, C. Batchelor-McAuley, R. G. Compton. *Phys. Chem. Chem. Phys.* 2017, **19**, 28-43.
- 9 T. Albrecht, S. Horswell, L. K. Allerston, N. V. Rees, P. Rodriguez. *Curr. Opin. Electrochem.* 2018, **7**, 138-145.
- 10 M. Pumera. *ACS Nano* 2014, **8**, 7555-7558.
- 11 Z.-P. Xiang, H.-Q. Deng, P. Peljo, Z.-Y. Fu, S.-L. Wang, D. Mandler, G.-Q. Sun, Z.-X. Liang. *Angew. Chem. Int. Ed.* 2018, **57**, 3464-3468.
- 12 Y. G. Zhou, N. V. Rees, R. G. Compton. *Angew. Chem. Int. Ed.* 2011, **50**, 4219-4221.
- 13 X. Jiao, S. V. Sokolov, E. E. L. Tanner, N. P. Young, R. G. Compton. *Phys. Chem. Chem. Phys.* 2017, **19**, 64-68.
- 14 S. Trasatti, O. A. Petrii. *I.U.P.A.C.* 1991, **63**, 711.
- 15 V. Climent, J. M. Feliu. *J. Solid State Electrochem.* 2011, **15**, 1297.
- 16 C. Jackson, G. T. Smith, D. W. Inwood, A. S. Leach, P. S. Whalley, M. Callisti, T. Polcar, A. E. Russell, P. Levecque, D. Kramer. *Nat. Commun.* 2017, **8**, 15802.
- 17 D. He, L. Zhang, D. He, G. Zhou, Y. Lin, Z. Deng, X. Hong, Y. Wu, C. Chen, Y. Li. *Nat. Commun.* 2016, **7**, 12362.
- 18 R. Dasari, D. A. Robinson, K. J. Stevenson. *J. Am. Chem. Soc.* 2013, **135**, 570-573.
- 19 X. Jiao, C. Batchelor-McAuley, C. Lin, E. Kätelhön, E. E. L. Tanner, N. P. Young, R. G. Compton. *ACS Catal.* 2018, **8**, 6192-6202.
- 20 W. Sheng, Z. Zhuang, M. Gao, J. Zheng, J.-G. Chen, Y. Yan. *Nat. Commun.* 2015, **6**, 5848.
- 21 E. Herrero, L. J. Buller, H. D. Abruña. *Chem. Rev.* 2001, **101**, 1897-1930.

- 22 S. E. F. Kleijn, B. Serrano-Bou, A. I. Yanson, M. T. M. Koper.  
*Langmuir* 2013, **29**, 2054-2064.
- 23 E. Wilhelm, R. Battino, R. J. Wilcock. *Chem. Rev.* **1977**, 77,  
219-262.
- 24 X. Li, C. Batchelor-McAuley, L. Shao, S. V. Sokolov, N. P.  
Young, R. G. Compton. *J. Phys. Chem. Lett.* 2017, **8**, 507-511.